

Article

Compression Properties and Its Prediction of Wood-Based Sandwich Panels with a Novel Taiji Honeycomb Core

Jingxin Hao ^{1,2}, Xinfeng Wu ^{1,*}, Gloria Oporto-Velasquez ², Jingxin Wang ² and Gregory Dahle ²

¹ College of Material Science and Engineering, Central South University of Forestry and Technology, Changsha 410018, China; haojingxin1@163.com

² Division of Forestry and Natural Resources, West Virginia University, WV 26506, USA; gloria.oporto@mail.wvu.edu (G.O.-V.); Jingxin.wang@mail.wvu.edu (J.W.); Gregory.dahle@mail.wvu.edu (G.D.)

* Correspondence: t20172345@csuft.edu.cn

Received: 27 June 2020; Accepted: 12 August 2020; Published: 15 August 2020



Abstract: The transverse compression property is one of most important aspects of the mechanical performance of a sandwich structure with a soft core. An experiment, analytical method and three digital strain measurement systems were applied to investigate the compression behavior and the failure mechanism for a wood-based sandwich structure with a novel Taiji honeycomb core. The results show that the structure of the Taiji honeycomb can improve dramatically on compression strength and modulus of composite compared to that of a traditional hexagonal one. There was no obvious deflection in the transverse direction detected by the three digital images before the buckling of the honeycomb occurred. An analytical equation between the key structure parameters and properties of the composite were applied to predict its threshold stresses and modulus. The properties of the core determine the strength of the entire structure, but the compression strength decreases slightly with an elevated core thickness, and its effect on the compression modulus can be neglected. Both the surface sheets and loading speed have little impact on the compression strength and modulus, respectively.

Keywords: wood-based sandwich composite; Taiji honeycomb; compression; deformation and failure

1. Introduction

Wood-based panels, such as medium density fiber board, particle board, and plywood, are extensively used in the furniture, interior furnishing and packaging product industries, etc. However, those materials fabricated based on formaldehyde-containing glue are harmful to human health and difficult to handle and recycle after usage [1]. One of the effective ways to void or reduce formaldehyde emissions is to find an alternative material to partially replace the formaldehyde-containing board. A honeycomb sandwich composite that is composed of two external thin faces and a large cellular core is an option. Thus, the composite can reduce the usage of formaldehyde-containing materials, which would only be applied as face sheets. Because of their high stiffness-to-weight and strength-to-weight ratios, sandwich composites have been recently receiving great attention [2–6]. However, the diverse raw materials used in the face and core layers of a sandwich composite make their mechanical properties, such as strength and deformation, more complex than homogeneous ones [7–10].

Previous theoretical and experimental studies have examined the failure behavior of sandwich composites made by metal, carbon or plastic. Meng et al. [11] demonstrated that, under out-of-plane compression, a graphene honeycomb exhibits two critical deformation events, such as elastic mechanical

instability (including elastic buckling and structural transformation) and inelastic structural collapse. Zhang et al. [12] performed in-plane compression and out-of-plan nano-indentation tests on the 3D honeycombs and revealed the localized collapse and significant plastic deformation of the honeycomb lattice, respectively. Daniel et al. [13] found the face yield in sandwich beams with carbon/epoxy facings and an aluminum honeycomb core loaded in a four-point bending test. Ashby et al. [14] generated collapse mechanism maps for sandwich composites in bending to show the dependence of the failure mode upon the geometry of the beam and the relative strength of the faces and core. These composites included aluminum alloy face-sheets and polymeric foam-cores, or metallic face-sheets and metallic foam-cores. To make an accurate prediction of the static failure loads and modes, others attempted to consider a local deflection effect near the loading point [15–17].

However, few studies have addressed the sandwich structure composed of a paper honeycomb core and wood-based skin. Cheng and Yan [18] investigated the influence of the thicknesses of a kraft paper honeycomb core on the stiffness of the sandwich panel by employing finite element models. They found that a decrease in the thickness ratio of the core-to-skin layer resulted in an increase in the modulus of elasticity and shear modulus of the sandwich panels. Hao et al. [19] comprehensively analyzed the deformation and failure mechanism of a wooden sandwich beam with a paper honeycomb core under a three-point bending test, and set up a method to optimize the strength-to-weight ratio of the composite. Wang and Bai [20] carried out dynamic experiments under a medium and low strain rate. A mechanical model was given to estimate the plateau stress and yield stress by employing the Cowper–Symonds model and a piecewise function. Other researches focused on the elastic properties of the paper-based cellular structures [21,22].

There are still some limitations on the use of a paper honeycomb as a core in sandwich composites, mostly related to their load-bearing resistance [18,20]. Si [23] developed a hexagonal honeycomb fortified by wooden strips with improved compression strength; however, due to the composite complexity and high production costs, the composite was not commercially successful. Developing a new honeycomb construction with a high strength is critical to improve the total mechanical properties of this kind of sandwich composite. So, the main goal of this research was to continue to investigate the compression properties of a new light-weight and cost-effective type of sandwich composite constituted by a Taiji honeycomb core between two layers of wood-based skins [24]. Three digital strain measurement systems were also used to analyze the failure procedure. In the end, the Taiji honeycomb was compared to a traditional hexagonal one to address the resistance difference under compression loading.

2. Experimental Programs

2.1. Test Materials and Properties

The sandwich composites prepared for the test comprised of wood-based face sheets and a paper honeycomb core. Medium-density fiberboard (MDF) with a thickness of 3.175 mm, plywood (PLY, hardwood) with a thickness of 3.175 mm and plywood with a thickness of 6.35 mm were selected as the face sheets while the traditional hexagonal and Taiji honeycombs (Figure 1) were used as the core layer of the composite, which is same as the materials used in the literature of Hao et al. [24]. The properties of those materials, tested according to ASTM D 1037-06a [25], are summarized in Tables 1 and 2 [24]. The adhesive was polyvinyl acetate (PVAc) from Franklin International Company, Columbus, USA, which was applied to attach the surface layers and the correspondent honeycomb core and to join the craft paper together to form a honeycomb structure. The Taiji honeycomb and sandwich structure were made in the laboratory; the detailed process and technique was same as in the literature [24].

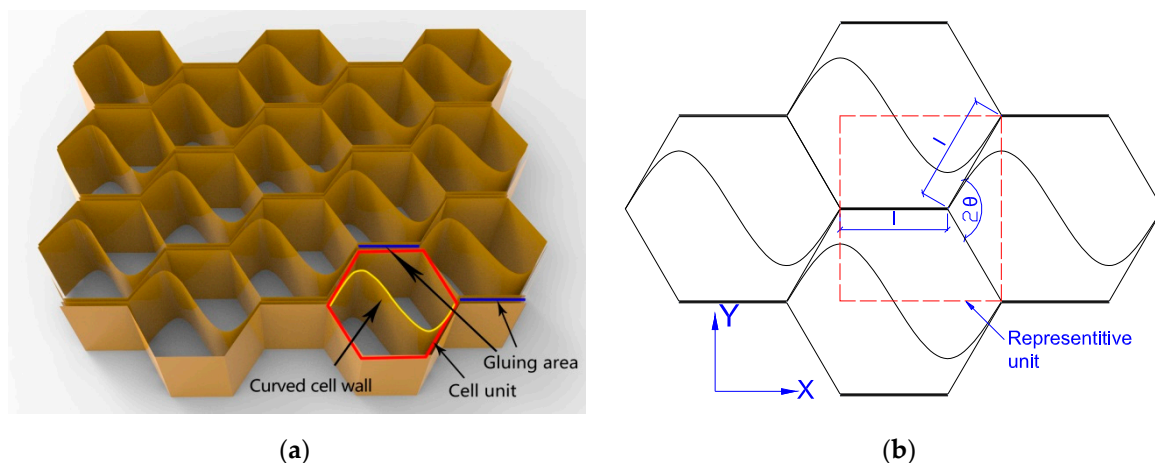


Figure 1. The structure of the Taiji honeycomb core: (a) three-dimensional picture; (b) two-dimensional picture ($l = 9.53$ mm and $2\theta = \frac{2\pi}{3}$).

Table 1. Properties of the medium-density fiberboard (MDF) and plywood (PLY) used in the outer layers (skins).

Material	Thickness (mm)	Density (g/cm ³)	Moisture Content (%)	Bending Strength (MPa)	Bending Modulus (MPa)
MDF	3.18	0.88	5.4	28.9	5399.9
PLY*	3.18	0.69	5.6	88.2	20,578.0
PLY*	6.35	0.68	5.4	64.2	13,598.7

* The properties were tested along the grain direction of outer layer of the PLY.

Table 2. Paper characteristics to fabricate the honeycomb core.

Material	Thickness (mm)	Moisture Content (%)	Tensile Strength (MPa)	Tensile Modulus (MPa)
Kraft paper	0.178	5.4	13.2	453.02

2.2. Test Methods

Specimens of the novel sandwich structure, with a combination of various face sheets and core thicknesses, were put under out-of-plane compression. A total of seven groups of tests were completed on the sandwich panels, with three kinds of surface sheets (A1: 3.18 mm MDF; A2: 3.18 mm PLY; and A3: 6.35 mm PLY) and three core thicknesses (B1: 15.9 mm; B2: 25.4 mm; and B3: 34.9 mm), as well as at three different loading speeds (C1: 0.5 mm/min; C2: 1.5 mm/min; and C3: 2.5 mm/min) (Table 3). Test Groups 1, 2 and 3 were carried out to evaluate the effect of core thickness on the compression properties of the sandwich structure. Test Groups 2, 4 and 5 were used to assess the effect of the surface sheet on the compression properties of the sandwich structure. Test Groups 5, 6 and 7 were applied to analyze the effect of the loading speed on the compression properties of the sandwich structure. A significant effect level ($p = 0.05$) of the thickness of the honeycomb core, surface sheets and loading speed on both the compression strength and modulus of composite, respectively, was checked by one-way ANOVA. In addition, to address the strength advantage of the Taiji honeycomb, Group 8, the traditional hexagonal honeycomb, was also tested and compared to the novel one. Three to five pieces were replicated to validate the results for each test group using a universal test machine, in which the displacement of the loading head was monitored automatically by the control system. In order to precisely observe the deformation and failure process of the samples under compression, a three-dimensional digital measurement system was used to record the strain distribution [26]. A fast-speed camera with Aramis software and a sensor system were used to trace

and calculate the dimension and shape change of the dark dot above the white paint background surface of the specimens (Figure 2).

Table 3. Experimental combinations of the sandwich beam structure parameters.

Group	Honeycomb	Code	Effective Replicate No.	Surface Sheet (A)	Core Thickness (B) (mm)	Loading Speed (C) (mm/min)
1	Taiji	A1B1C1	5 for strength 3 for modulus	3.18 mm MDF (A1)	15.9 (B1)	0.5 (C1)
2	Taiji	A1B2C1	4 for strength 3 for modulus	3.18 mm MDF (A1)	25.4 (B2)	0.5 (C1)
3	Taiji	A1B3C1	3 for strength 3 for modulus	3.18 mm MDF (A1)	34.9 (B3)	0.5 (C1)
4	Taiji	A2B2C1	5 for strength 5 for modulus	3.18 mm PLY (A2)	25.4 (B2)	0.5 (C1)
5	Taiji	A3B2C1	3 for strength 3 for modulus	6.35 mm PLY (A3)	25.4 (B2)	0.5 (C1)
6	Taiji	A3B2C2	3 for strength 3 for modulus	6.35 mm PLY (A3)	25.4 (B2)	1.5 (C2)
7	Taiji	A3B2C3	3 for strength 3 for modulus	6.35 mm PLY (A3)	25.4 (B2)	2.5 (C3)
8	Hexagonal	A1B2C1	4 for strength 5 for modulus	3.18 mm MDF (A1)	25.4 (B2)	0.5 (C1)



(a)



(b)

Figure 2. Three-dimensional digital measurement system. (a) Measurement set-up; (b) paint on the surface of the specimens.

3. Theoretical Analysis and Prediction

3.1. Strength Calculation of the Taiji Honeycomb

Honeycomb can be recognized as periodic cell construction constituted by a thin wall, so that the strength of the structure is not decided by its strength of material, but by the buckling stress of the thin wall. In other words, the cell collapse can be recognized as the buckling of the interconnected thin wall through a specific constraint between the honeycomb prisms under transverse compression.

The buckling stress of the thin wall was given by Timoshenko [27]; that is Equation (1),

$$\sigma_{pc} = \frac{K_c E_s}{(1 - \nu_s^2)} \left(\frac{t}{l}\right)^3 \quad (1)$$

where σ_{pc} denote the compression buckling stress of the cell wall; E_s and ν_s are the transverse modulus and Poisson's ratio of the cell wall, respectively; t and l are, respectively, the thickness and width of the cell edge; and K_c is an end constraint factor.

Consider an idealized structure of the Taiji honeycomb with a cell size l , edge thickness t and angle 2θ between the inclined edge, as depicted in Figure 1b. Selecting the representative unit of the Taiji cells, the equivalent compress buckling stress can be expressed as Equation (2) [24],

$$\sigma_{tc} = \frac{17.5}{(1 + \cos\theta)\sin\theta} \frac{K_c E_s}{(1 - \nu_s^2)} \left(\frac{t}{l}\right)^3 \quad (2)$$

where σ_{tc} denotes the compression buckling stress of the Taiji honeycomb.

3.2. Modulus Calculation of the Taiji Honeycomb

The equivalent compression modulus of a representative cell of the Taiji honeycomb that was derived from its geometrical parameters and characteristics of the kraft paper is Equation (3) [24],

$$E_{tc} = \frac{4}{(1 + \cos\theta)\sin\theta} \frac{t}{l} E_s \quad (3)$$

where E_{tc} is the compression modulus of the Taiji honeycomb by prediction; and E_s is the Yang modulus of the kraft paper.

It was not calculated directly from the compression test due to the skin effect of the sandwich composite. However, the average modulus of the whole entire structure can be obtained from the test according to the following Equation (4) (Figure 3),

$$E_c = \frac{h \Delta p}{s \Delta h} \quad (4)$$

where Δp and Δh are the load and displacement increments in the elastic stage, respectively; E_c is the average compression modulus of the entire structure; and s and h are the horizontal cross-sectional area and height of the sandwich structure, respectively.

When the sandwich structure is loaded by transverse compression, the total displacement is the sum of the surface sheets of the outer layer and the honeycomb in the core (Equation (5)).

$$\varepsilon_c h = 2\varepsilon_{fc} h_f + \varepsilon_{cc} h_c \quad (5)$$

where ε_c , ε_{fc} and ε_{cc} denote the compression strain of the entire structure, surface sheets and core layer, respectively; and h_f and h_c are the skin and core thickness, respectively. It should be noted that h_c is also the height of the cell wall of the honeycomb.

Using Hook's law, Equation (5) is converted to Equation (6),

$$\frac{\sigma_c}{E_c} h = \frac{\sigma_c}{E_{fc}} 2h_f + \frac{\sigma_c}{E_{cc}} h_c \quad (6)$$

where σ_c is the transverse stress; and E_{fc} and E_{cc} denote the compression modulus of the skin and core, respectively.

After several arrangements, Equation (6) was expressed as Equation (7),

$$E_{cc} = \left(\frac{E_{cc}}{E_{fc}} \frac{2h_f}{h} + \frac{h_c}{h} \right) E_c \quad (7)$$

Due to $E_{cc} \ll E_{fc}$ and $h_f < h$, $\frac{E_{cc}}{E_{fc}} \frac{2h_f}{h} \approx 0$. Equation (7) was simplified as Equation (8),

$$E_{cc} = \frac{h_c}{h} E_c \quad (8)$$

Integrating Equation (4) into Equation (8), we can get Equation (9),

$$E_{cc} = \frac{h_c}{s} \frac{\Delta p}{\Delta h} \quad (9)$$

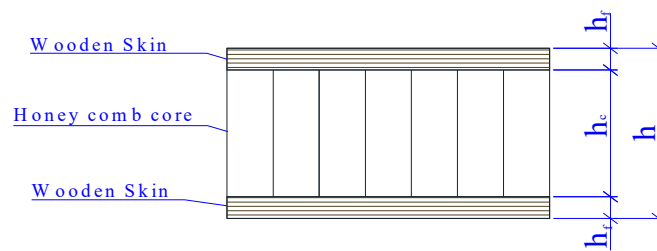


Figure 3. Notation of the sandwich structure with the Taiji honeycomb core.

4. Result and Discussion

4.1. Deformation and Failure Process

Figure 4 exhibits a typical stress–strain curve of the sandwich structure with a Taiji honeycomb core under out-of-plane compression. The deformation and failure process can be approximately categorized into four stage, namely, I, II, III and IV. In the first stage, I, the correlation between the stress and strain was almost linear, which confirmed Hook's law. The loading increased lineally until the compression stress of the honeycomb was attained at the buckling point of the single-layer cell wall, the curve goes into the stage II, denoted as the non-elastic stage. In this stage, the ribbon cell wall (triple-layer wall) remains to carry increasing stress, while the inclined cell wall (single-layer wall) only takes a partial buckling load. The initiation of significant deformation of the inclined cell wall was observed from photographs while the strain was not clearly demonstrated along the transverse direction of the sandwich structure from the digital image (Figure 5b). Then the stress continued to elevate non-linearly to the maximum point until the ribbon wall started to buckle. As stage III started, the stress dropped by a large amount after the peak stress, as well as the large strain measured. After that, the stress went into a plateau, maintaining it for a long period of time, called stage IV. According to research of Wang et al. [28], the stress will go up again when the honeycomb structure was densified under compression.

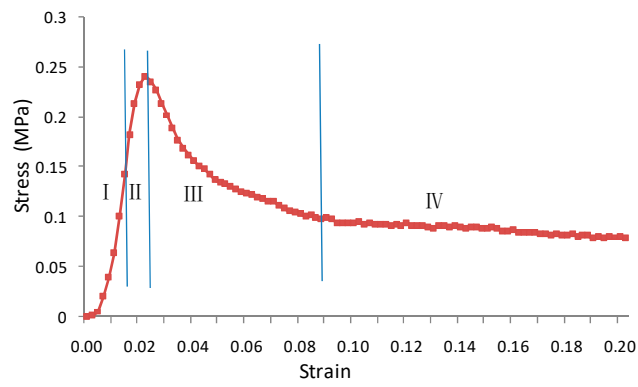
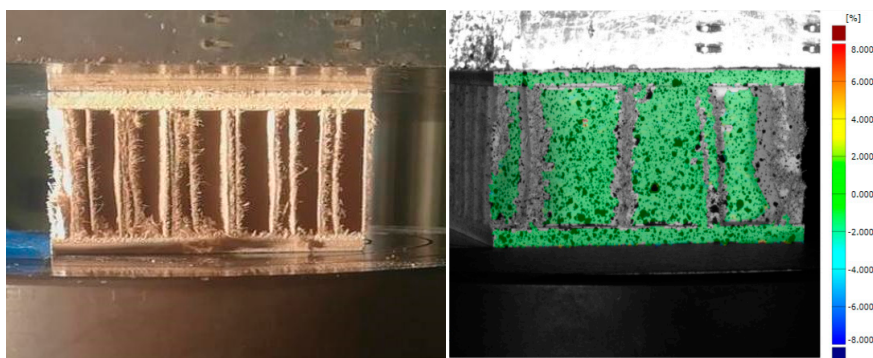
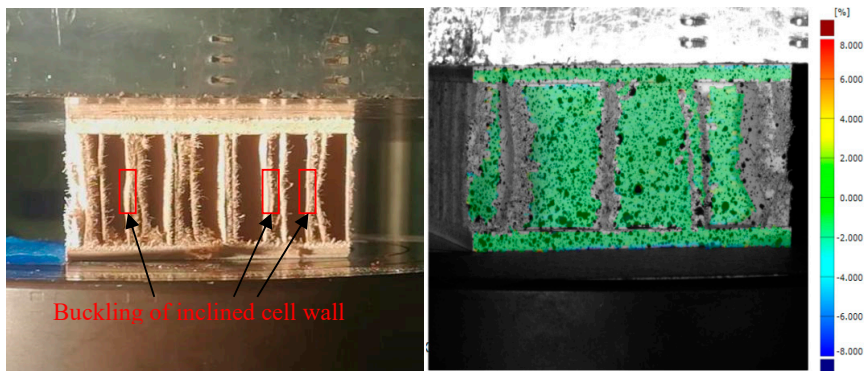


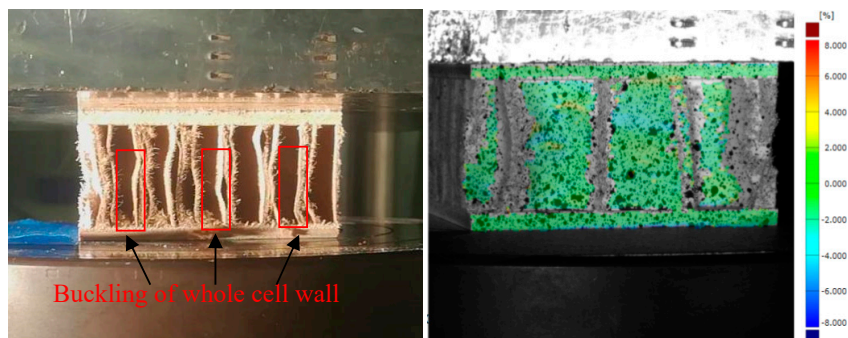
Figure 4. Typical stress–strain curves of sandwich structure with a Taiji honeycomb core under out-of-plane compression.



(a)



(b)



(c)

Figure 5. Cont.

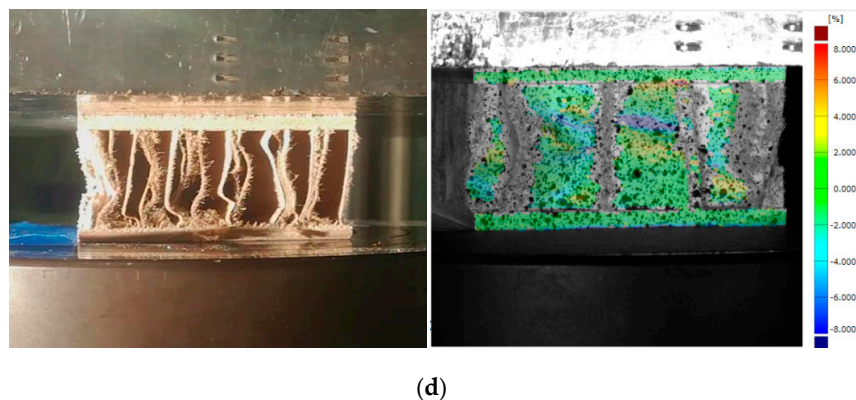


Figure 5. Photographs and digital image of the sandwich structure with a Taiji honeycomb core under compression: (a) unloaded; (b) buckling of the inclined cell wall; (c) buckling of the whole cell wall; (d) the plateau stage. The red box on the left of pictures (b) and (c) expresses the deformed process of the cell wall in the honeycomb core. The colored scale on the right of the pictures is the strain distribution along the cross section of the composite.

4.2. Strength Comparison between the Theoretical Calculation and Measured Results

The predicted strength derived by the cell wall characteristics and the measured results of the sandwich structure under transverse compression are summarized in Table 4. The failure was taken to be the maximum load carried by the specimen before the abrupt load drop and coincident with the observation of a clearly evident failure. Compression buckling of the honeycomb core was observed in this experiment, which decided the entire strength of the sandwich structure. Equation (2) was applied to calculate the predicted results. Poisson's ratio $\nu_s = 0.3$ and $\theta = \frac{\pi}{3}$ are used in Equation (2); the characteristics of the kraft paper as the input parameters are from Table 2 while the constraint factor K_c was decided by following the method. Considering the honeycomb structure glued outside to a wood-based panel, the constraint between the cell wall is neither completely free nor rigidly clamped while the connection between the cell and panel is recognized as clamped (Gibson (1999)). As an approximation, $K_c = 5.0$ was used in this paper.

Table 4. Predicted strength derived by the cell wall characteristics and measured results of the sandwich structure under transverse compression.

Group	Code	Surface Sheet (A)	Core Thickness (B) (mm)	Loading Speed (C) (mm/min)	Measured Value (MPa)	Standard Deviation (MPa)	Predicted Value (MPa)
1	A1B1C1	3.18mm MDF (A1)	15.9 (B1)	0.5 (C1)	0.24	0.03	0.22
2	A1B2C1	3.18mm MDF (A1)	25.4 (B2)	0.5 (C1)	0.23	0.02	0.22
3	A1B3C1	3.18mm MDF (A1)	34.9 (B3)	0.5 (C1)	0.21	0.11	0.22
4	A2B2C1	3.18mm PLY (A2)	25.4 (B2)	0.5 (C2)	0.21	0.03	0.22
5	A3B2C1	6.35mm PLY (A3)	25.4 (B2)	0.5 (C1)	0.23	0.01	0.22
6	A3B2C2	6.35mm PLY (A3)	25.4 (B2)	1.5 (C2)	0.23	0.01	0.22
7	A3B2C3	6.35mm PLY (A3)	25.4 (B2)	2.5 (C3)	0.24	0.04	0.22

4.3. Modulus Comparison between the Theoretical Calculation and Measured Results

Table 5 exhibits the predicted modulus derived by the cell wall characteristics and measured values of the sandwich structure under transverse compression. The measured results were calculated by Equation (9) on the basis of the test data obtained in the elastic stage of the deformation while the predicted values were obtained by Equation (3); all the input parameters of the kraft paper are from Table 2. The predicted value exceeded the measured results of the specimens with various core thicknesses, surface sheets and loading speeds. The possible reason is that the compression modulus of the honeycomb is sensitive to its cell walls evenness. However, the theoretical evenness of all the cell walls were not kept very well due to the process accuracy, so that a few of the cell walls of the specimens were deformed before the test.

Table 5. Predicted modulus derived by the cell wall characteristics and measured results of the sandwich structure under transverse compression.

Group	Code	Surface Sheet (A)	Core Thickness (B) (mm)	Loading Speed (C) (mm/min)	Measured Value (MPa)	Standard Deviation (MPa)	Predicted Value (MPa)
1	A1B1C1	3.18mm MDF (A1)	15.9 (B1)	0.5 (C1)	23.00	3.13	26.04
2	A1B2C1	3.18 mm MDF (A1)	25.4 (B2)	0.5 (C1)	22.32	2.02	26.04
3	A1B3C1	3.18 mm MDF (A1)	34.9 (B3)	0.5 (C1)	24.83	1.60	26.04
4	A2B2C1	3.18 mm PLY (A2)	25.4 (B2)	0.5 (C2)	21.11	3.54	26.04
5	A3B2C1	6.35 mm PLY (A3)	25.4 (B2)	0.5 (C1)	24.38	4.87	26.04
6	A3B2C2	6.35 mm PLY (A3)	25.4 (B2)	1.5 (C2)	22.04	3.07	26.04
7	A3B2C3	6.35 mm PLY (A3)	25.4 (B2)	2.5 (C3)	22.35	3.45	26.04

4.4. The Effect of the Structure Parameters on the Compression Properties

The curve of strength and the modulus versus core thickness are presented in Figure 6. There is a slight decrease in the compression strength as the core thickness rises. As the core thickness increased from 15.9 mm to 34.9 mm, the compression strength dropped by 12.5%. The compression modulus almost keeps steady with different core thickness. Various surface sheets also have little effect on both the compression strength and modulus, which confirms the decisive role of the core layer of honeycomb to the entire structure properties (Figure 7). Figure 8 exhibits that the same level of compression strength and modulus was obtained at various loading speeds from 0.5 mm/min to 2.5 mm/min. So, the test can be recognized as quasi-static compression during that speed range.

The variance analysis and statistical values are also coinciding with the graphic interpretation depicted from Figures 6–8. A significant effect level ($p = 0.05$) of the thickness of the honeycomb core, surface sheets and loading speed on both the compression strength and modulus of composite, respectively, was not found (Table 6).

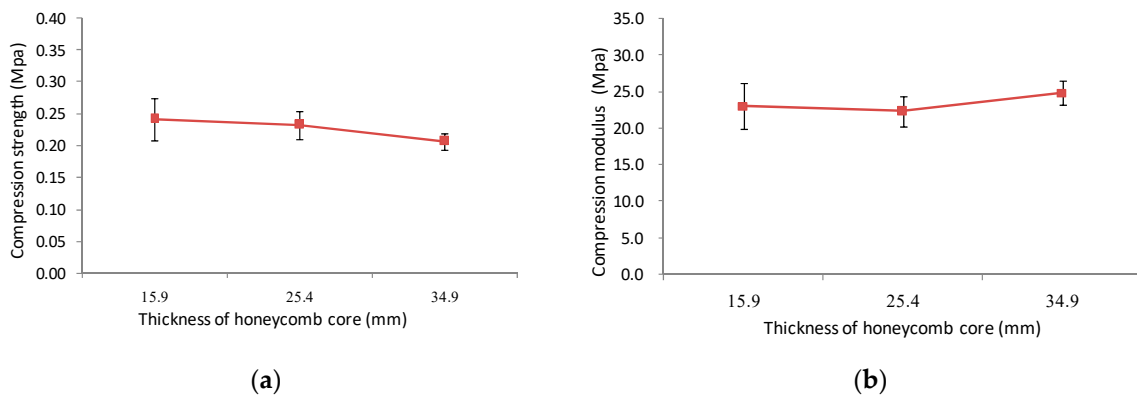


Figure 6. The effect of thickness of the honeycomb core on compression properties: (a) compression strength; (b) compression modulus (surface sheet: 3.18 mm MDF; loading speed: 0.5 mm/min; and vertical bar: error bar with standard deviation).

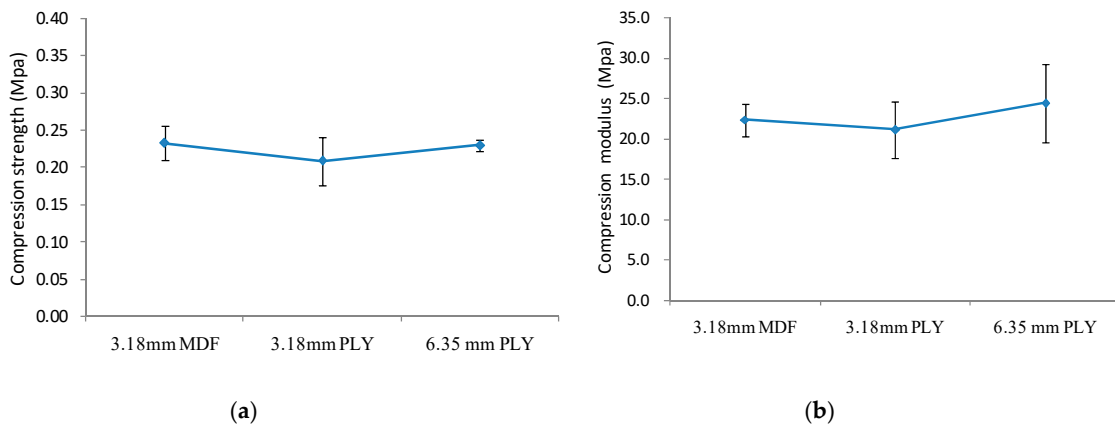


Figure 7. The effect of surface sheets on compression properties: (a) compression strength; (b) compression modulus (ore thickness: 25.4 mm; loading speed: 0.5 mm/min; and vertical bar: error bar with standard deviation).

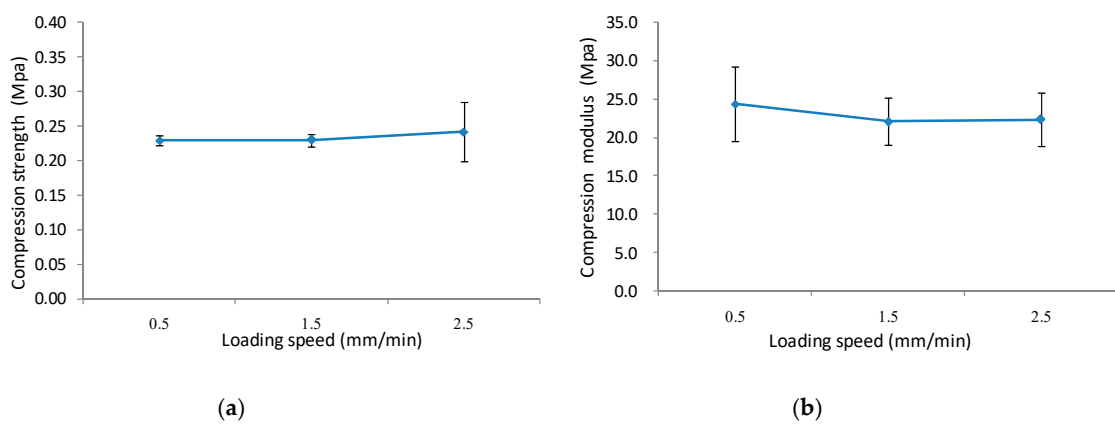


Figure 8. The effect of loading speed on compression properties: (a) compression strength; (b) compression modulus (surface sheet: 6.35 mm PLY; core thickness: 25.4 mm; and vertical bar: error bar with standard deviation).

Table 6. Variance analysis summary.

The Effect of Core Thickness on the Compression Strength.						
Variance Source	Sum of Squares	Degree of Freedom	Mean Squares	F Value	p Value	F Critical Value
Between group	0.0023	2	0.0012	1.45	0.29	F _{0.05} = 4.26
Internal group	0.0073	9	0.0008			
Sum	0.0096	11				
The Effect of Core Thickness on the Compression Modulus.						
Variance Source	Sum of Squares	Degree of Freedom	Mean Squares	F Value	p Value	F Critical Value
Between group	10.12	2	5.06	0.53	0.61	F _{0.05} = 5.14
Internal group	57.27	6	9.54			
Sum	67.39	8				
The Effect of Surface Sheets on the Compression Strength.						
Variance Source	Sum of Squares	Degree of Freedom	Mean Squares	F Value	p Value	F Critical Value
Between group	0.0016	2	0.0008	1.03	0.40	F _{0.05} = 4.26
Internal group	0.0069	9	0.0008			
Sum	0.0085	11				
The Surface Sheets on the Compression Modulus.						
Variance Source	Sum of Squares	Degree of Freedom	Mean Squares	F Value	p value	F critical value
Between group	20.05	2	10.02	0.37	0.70	F _{0.05} = 4.46
Internal group	217.63	8	27.20			
Sum	237.68	10				
The Loading Speed on the Compression Strength.						
Variance Source	Sum of Squares	Degree of Freedom	Mean Squares	F Value	p Value	F Critical Value
Between group	0.0003	2	0.0002	0.15	0.86	F _{0.05} = 5.14
Internal group	0.0061	6	0.0010			
Sum	0.0064	8				
The Loading Speed on the Compression Modulus.						
Variance Source	Sum of Squares	Degree of Freedom	Mean Squares	F Value	p Value	F Critical Value
Between group	9.65	2	4.82	0.13	0.88	F _{0.05} = 5.14
Internal group	224.07	6	37.35			
Sum	233.72	8				

4.5. Comparison between Taiji the Honeycomb and Traditional Hexagonal Honeycomb

It is revealed in Figure 9 that the structure of the Taiji honeycomb can improve dramatically in the compression strength and modulus of the composite. Its compression strength and modulus is 2.45 times and 2.7 times, respectively, than that of traditional hexagonal honeycomb with the same cellular size. This is because every unit of the Taiji honeycomb has a curved paper inside of the cell and strengthens to three layers of paper between the cell boundaries, which enhances dramatically to stability of the thin wall of the cellular structure. However, the reinforcement of transverse compression properties observed in the experiments is lower than the theoretical calculation in the literature [24].

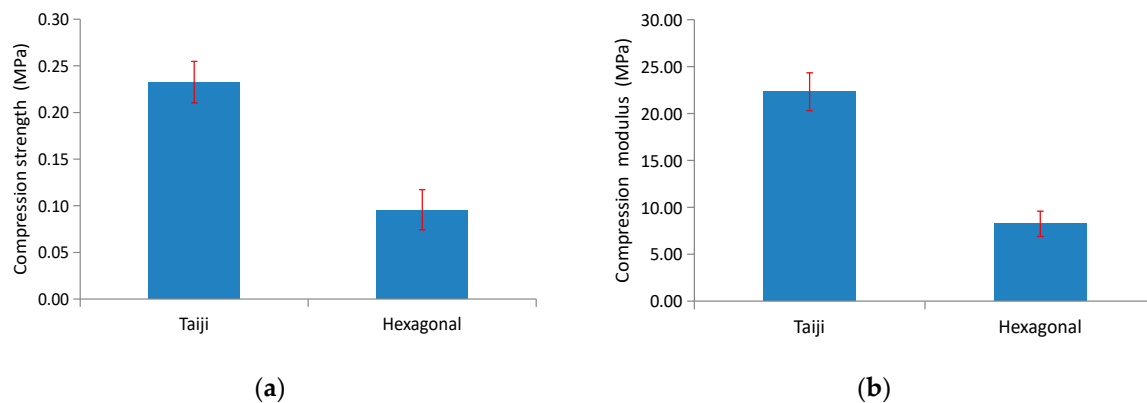


Figure 9. The properties of the Taiji honeycomb compared to the traditional hexagonal one: (a) compression strength; (b) compression modulus ($l = 9.5$ mm; $A = 3.18$ mm MDF; $B = 25.4$ mm; $C = 0.5$ mm/min; and vertical bar: error bar with standard deviation).

5. Conclusions

A new type of Taiji honeycomb was fortified on the basis of the traditional hexagonal ones, where in every unit a curve inside of the cell was added, strengthening the three layers of paper between cells boundaries. The compression strength and modulus of the Taiji honeycomb was 2.45 times and 2.7 times, respectively, that of the traditional hexagonal one.

There was no obvious deflection in the transverse direction detected by three digital images before the buckling of the honeycomb occurred. Thus, the compression properties of the sandwich structure, especially for modulus, are sensitive to the surface evenness of the honeycomb. An analytical equation between the key structure parameters and properties of the composite were applied to predict its threshold stresses and modulus, which had good coincidence with the measured results. The properties of the core decide the strength of the entire structure, but the compression strength decreases slightly with an elevated core thickness, and its effect on the compression modulus can be neglected. Both the surface sheets and loading speed have little impact on compression strength and modulus, respectively.

Author Contributions: J.H.: test plan, paper writing, modeling; X.W.: specimen preparation, testing, data collection and analysis; G.O.-V.: material purchase, testing support; J.W.: funding; G.D.: three digital image support. All authors have read and agreed to the published version of the manuscript.

Funding: This project was supported by the Key Research Project of Hunan Education Department (18A156) and China Scholarship Council (CSC).

Acknowledgments: The authors also thank David De Vallance for advice regarding specimen preparation.

Conflicts of Interest: The authors declare no conflict of interest.

References

- Zou, N.; Liang, L.P. Research advances on formaldehyde emission of wood-based panels. *Sichuan For. Explor. Des.* **2018**, *2*, 80–86.
- Wang, Z.G.; Li, Z.D.; Zhou, W.; Hui, D. On the influence of structural defects for honeycomb structure. *Compos. Part B* **2018**, *142*, 183–192. [[CrossRef](#)]
- Maslej, M.; Smardzewski, J. Experimental testing of elastic properties of LayWood pyramidal cores. *BioResources* **2019**, *14*, 9686–9703.
- Smardzewski, J.; Gajęcki, A.; Wojnowska, M. Investigation of elastic properties of paper honeycomb panels with rectangular cells. *BioResources* **2019**, *14*, 1435–1451.
- Smardzewski, J. Wooden sandwich panels with prismatic core—energy absorbing capabilities. *Compos. Struct.* **2019**, *230*, 111535. [[CrossRef](#)]
- Hao, J.X.; Wu, X.F.; Liu, W.J. Bending property of sandwich beam based on layer-wise first-order theory. *J. Build. Mater.* **2014**, *17*, 1049–1053.

7. Gibson, L.J.; Ashby, M.F. *Cellular Solids: Structure and Properties*, 2nd ed.; Cambridge University Press: Cambridge, UK, 1999.
8. Smardzewski, J.; Wojciechowski, K.W. Response of wood-based sandwich beams with three-dimensional lattice core. *Compos. Struct.* **2019**, *216*, 340–349. [[CrossRef](#)]
9. Hao, J.X.; Wu, X.F.; Liu, W.J. Modeling and verification of sandwich beam with wooden skin and honeycomb core subjected to transverse loading. *Sci. Silvae Sinicae* **2014**, *50*, 128–137.
10. Wu, X.F.; Xu, J.Y.; Hao, J.X. Calculating elastic constants of binderless bamboo-wood sandwich composite. *BioResources* **2015**, *10*, 4473–4484. [[CrossRef](#)]
11. Meng, F.C.; Cheng, C.; Hu, D.Y.; Song, J. Deformation behaviors of three-dimensional graphene honeycombs under out-of-plane compression: Atomistic simulations and predictive modeling. *J. Mech. Phys. Solids* **2017**, *109*, 241–251. [[CrossRef](#)]
12. Zhang, Z.; Kutana, A.; Yang, Y.; Krainyukova, N.V.; Penev, E.S.; Yakobson, B.I. Nanomechanics of carbon honeycomb cellular structures. *Carbon* **2017**, *113*, 26–32. [[CrossRef](#)]
13. Daniel, I.M.; Abot, J.L. Fabrication, testing and analysis of composite sandwich beams. *Compos. Sci. Technol.* **2000**, *60*, 2455–2463. [[CrossRef](#)]
14. Ashby, M.F.; Evans, A.G.; Fleck, N.A.; Gibson, L.J.; Hutchinson, J.W.; Wadley, H.N.G. *Metal Foams: A Design Guide*; Butterworth-Heinemann: London, UK, 2000.
15. Minakuchi, S.; Okabe, Y.; Takeda, N. Segment-wise model for theoretical simulation of barely visible indentation damage in composite sandwich beams: Part I—Formulation. *Compos. Part A Appl. Sci. Manuf.* **2008**, *39*, 133–144. [[CrossRef](#)]
16. Caprino, G.; Durante, M.; Leone, C.; Lopresto, V. The effect of shear on the local indentation and failure of sandwich beams with polymeric foam core loaded in flexure. *Compos. Part B Eng.* **2015**, *71*, 45–51. [[CrossRef](#)]
17. Lim, T.S.; Lee, C.S.; Lee, D.G. Failure modes of foam core sandwich beams under static and impact loads. *J. Compos. Mater.* **2004**, *38*, 1639–1662. [[CrossRef](#)]
18. Chen, Z.; Yan, N. Investigation of elastic moduli of kraft paper honeycomb core sandwich panels. *Compos. Part B* **2012**, *43*, 2107–2114. [[CrossRef](#)]
19. Hao, J.X.; Wu, X.F.; Oporto, G.; Liu, W.J.; Wang, J.X. Structural analysis and strength-to-weight optimization of wood-based sandwich composite with honeycomb core under three-point flexural test. *Eur. J. Wood Prod.* **2020**. [[CrossRef](#)]
20. Wang, D.M.; Bai, Z.Y. Mechanical property of paper honeycomb structure under dynamic compression. *Mater. Des.* **2015**, *77*, 59–64. [[CrossRef](#)]
21. Słonina, M.; Dziurka, D.; Smardzewski, J. Experimental research and numerical analysis of the elastic properties of paper cell cores before and after impregnation. *Materials* **2020**, *13*, 2058. [[CrossRef](#)]
22. Peliński, K.; Smardzewski, J. Experimental testing of elastic properties of paper and WoodEpoxy in honeycomb panels. *BioResources* **2019**, *14*, 2977–2994.
23. Si, L.L. Study on the mechanical properties of wood material enhanced paper honeycomb core composite boards. *For. Mach. Woodwork. Equip.* **2012**, *40*, 25–28.
24. Hao, J.X.; Wu, X.F.; Oporto, G.; Wang, J.X.; Dahle, G.; Nan, N. Deformation and failure behavior of wooden sandwich composite with Taiji honeycomb core under three-point bending. *Materials* **2018**, *11*, 2325. [[CrossRef](#)] [[PubMed](#)]
25. ASTM D 1037-06a. *Standard Test Methods for Evaluating Properties of Wood-Base Fiber and Particle Panel Materials*; ASTM International: West Conshohocken, PA, USA, 2011.
26. Dahle, G.A. Influence of bark on the mapping of mechanical strain using digital image correlation. *Wood Sci. Technol.* **2017**, *51*, 1469–1477. [[CrossRef](#)]
27. Timoshenko, S.P.; Gere, J.M. *Theory of Elastic Instability*; McGraw-Hill Publishing Company: New York, NY, USA, 1961.
28. Wang, Z.; Liu, J.; Hui, D. Mechanical behaviors of inclined cell honeycomb structure subjected to compression. *Compos. Part B* **2017**, *110*, 307–314. [[CrossRef](#)]

